Multi-objective Optimization of Peak Cutting Force and Cutting Energy Consumption in Cutting of *Caragana korshinskii* Branches

Yaoyao Gao,[a] Xiaoya Hu,[b] Siyuan Tong,[a] Jiangming Kan,[a] Yutan Wang,[b] and Feng Kang [a,*]

Caragana korshinskii (C.K.) flat stubble residue is an abundant biomass energy source in China. Because branch cutting is closely related to the harvesting of forest biomass, it is practical for forestry production and ecological development to investigate the effects of cutting parameters on the peak cutting force and cutting energy consumption of C.K. branches. In this study, the effect of cutting parameters on the peak cutting force and cutting power consumption of branches was investigated by single-factor and multi-factor tests using an independently developed reciprocating cutting test bench, and an optimization model was established. The interaction term of average cutting speed and tool cutting edge inclination angle significantly affected the peak cutting force, while the interaction term of cutting clearance and wedge angle had a significant effect on the cutting energy consumption. The optimal combination of cutting parameters was an average cutting speed of 0.5 m/s, cutting clearance of 1.4 mm, wedge angle of 25°, and tool cutting edge inclination angle of 20°. With this combination of parameters, the corresponding peak cutting force was 644.38 N, and the cutting energy consumption was 5.90 J, which was less than 5% relative error between each performance index and the theoretical optimized value.

Contact information: a: School of Technology, Beijing Forestry University, Beijing 100083, China; b: School of Mechanical Engineering, Ningxia University, Yinchuan 750021, China;
* Corresponding author: kangfeng98@bjfu.edu.cn

INTRODUCTION

Caragana korshinskii (C.K.) is a tree of the Pteridophyllaceae family. It is a deciduous shrub, mainly distributed in Loess Plateau and Northwest desert areas in China, with the characteristics of drought resistance, cold resistance, heat resistance, and sand burial resistance (Waseem *et al*. 2021; Che *et al*. 2022). It is a high-quality shrub fodder plant resource with high ecological and economic value (Wang *et al*. 2021). The use of C.K. branches as raw material for biomass power generation can alleviate the problem of energy constraints, reduce environmental pollution caused by burning fossil energy, and improve the energy utilization system (Xu *et al*. 2020). However, it is difficult to cut the phloem of the branches, which increases the time and energy consumption of the cutting process. This difficulty affects the operating efficiency of the cutting device and the cost of biomass energy generation (Suzuki *et al*. 2017).

bioresources.com

The cutting process of different plant stems is closely related to their material properties, the structure of the cutting parts, and the kinematic parameters, which affect their mechanical properties (Liu *et al*. 2020). The influence of material properties of stalks on cutting mechanical properties has been reported mainly for cutting tests with stalk parts (Aydin and Arslan 2018; Esgici 2020), moisture content (Zhang *et al*. 2019), and stem cross-sections (Mathanker *et al*. 2015) as test factors, all of which affect the mechanical properties of stalk cutting. In addition to the material properties of the stalk, structural parameters of the cutting components influence the mechanical properties of the stem using the combination form of cutting blades (Gan *et al*. 2018), cutting type (Qiu *et al*. 2021) and tool parameters (Atkins 2009; Gao *et al*. 2022). The cutting power consumption can be reduced in the case of oblique cutting of stems (Zhang *et al*. 2022). To examine the influence of cutting part motion parameters on the mechanical properties of stalks, the stalk cutting test bench has been developed to analyze the influence of cutting speed and stalk feeding speed (Wang *et al*. 2021). Cutting speed has a significant influence on stalk cutting force and power consumption (Vu *et al*. 2020).

The cutting force and cutting energy consumption of plant stems are closely related to the cutting device tool parameters and motion parameters. Most studies have been conducted for single-knife impact cutting, or universal testing machine cutting tests in low-speed modes (Cristovao *et al*. 2013). If the cutting speed is high, then the cutting energy consumption may be high even with a small cutting force (Kakahy *et al*. 2014). Therefore, it is desirable to reduce both cutting force and cutting power consumption. For the cutting performance of C.K. branches, Gao *et al.* (2021) investigated the effect of cutting parameters on peak cutting force during supported and unsupported cutting using a self-designed pendulum cutting test stand. Since the pendulum cutting test bench uses the inertial force of the pendulum to cut the branches, its cutting speed is high, while the operating speed of the tool cannot be achieved in the actual operation process. To solve the above problems, this study takes the single C.K. branch as the test object, using the branch diameter (D), average cutting speed (v), cutting clearance (c), wedge angle (β), tool cutting edge inclination angle (λ), and moisture content (W) as the test factors, with the peak cutting force (F) and cutting energy consumption (E) as the test objectives. The influence of each factor on the test objectives was investigated, and the optimal combination of cutting parameters provides a reference for the optimal design of the branch cutting mechanism.

EXPERIMENTAL

Test Materials

The material for this experiment was collected from Yanchi, Ningxia (38°6′21.71″N, 106°52′29.37″E), in August 2020, at the age of 5 years. The branches without nodes, diseases, or insects were randomly selected, with diameters ranging from 6 to 20 mm and lengths of 150 mm. With good toughness and wear resistance, Cr12MoV is chosen as the material for cutting tools. According to GB/T 1299-2014, the chemical composition content of Cr12MoV is of C 1.45 to 1.70%, Si ≤0.4%, Mn ≤0.4%, Cr 11.0 to 12.5%, Mo 0.40 to 0.60%, V 0.15 to 0.30%, S ≤0.03%, and P ≤0.03%. The heat treatment process of Cr12MoV is that the material is firstly heated in the range 950 to 1000 °C and then quenched in oil cooling for 20 minutes. After that, it is tempered at 520 °C two times to achieve its material hardness value of ≥ 60HRC. The retrieved branches were wrapped

bioresources.com

in sealed bags and refrigerated to prevent changes in moisture content, which was determined within 24 h of the branch cutting test.

Equipment

The reciprocating cutter is composed of a moving knife and a fixed knife to complete the cutting. According to its working principle, the team designed a branch reciprocating cutting test bench, as shown in Fig. 1.
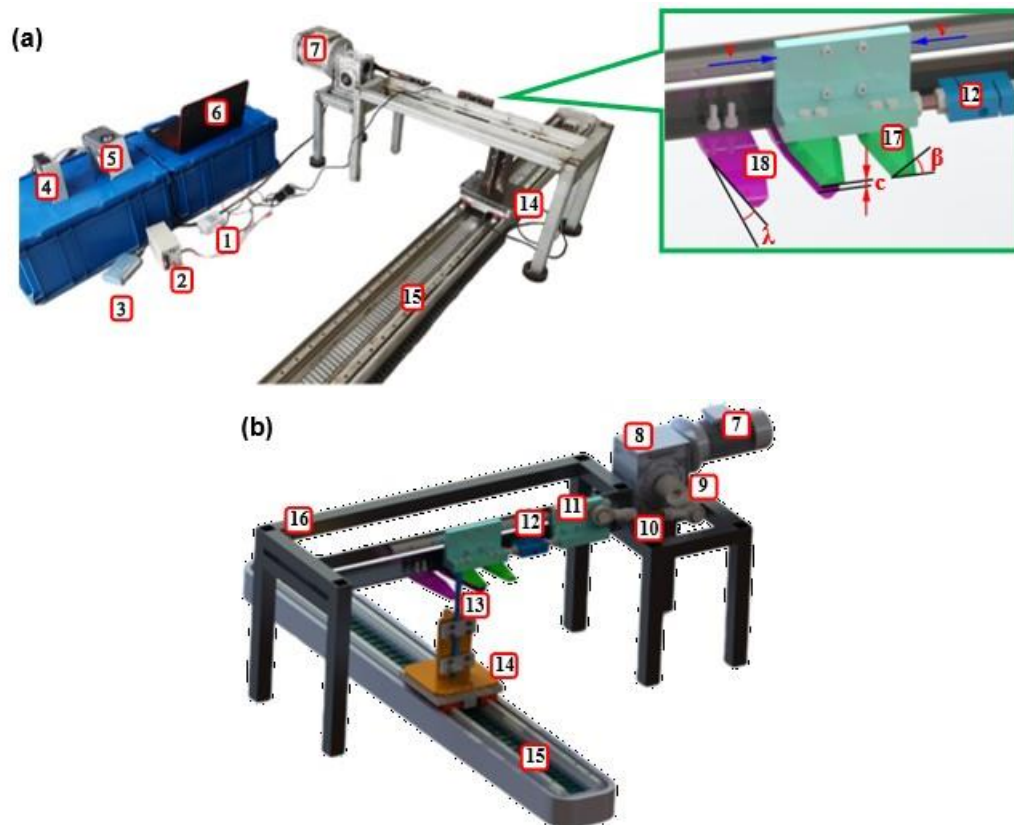
1-Amplifier; 2-24V DC power supply; 3-MCC-1608G acquisition card; 4-Linear motor controller; 5- Variable-frequency Drive; 6-Computer; 7-Motor; 8-Reducer; 9-Crank; 10-Connecting rod; 11-Moving slider; 12- S-type tension pressure sensor; 13- *Caragana korshinskii* branch; 14-branch clamp; 15-Flat linear motor; 16- cutting table frame; 17-Fixed blade; 18-Moving blade

Fig. 1. Cutting test bench

The cutting table frame consists of crank slider mechanism, inverter, AC motor, reducer, cutting tool, and frame. The crank slider mechanism is driven by an AC motor through a reducer (Fig. 1b). The AC motor is controlled by a Variable-frequency Drive to control the speed. The slider section consists of double sliders connected in series. A s-type tension sensors (Dysensor Co., Ltd., Bengbu, China) with measurement range of 5000 N and accuracy of ±0.5% is connected in series between the two sliders to detect the branch cutting force. The moving blade is connected with the slider, the fixed knife is fixed on the frame, and the slider moves along the slide to realize reciprocating cutting of branches. The branch feeding mechanism includes a flat linear motor, and a branch clamp. The branch clamp is fixed to the mover of the flat linear motor. When the crank speed is stable, the branches are fed at a constant speed by controlling the linear motor controller. Referring to

the operating efficiency of the forage harvester (Gao *et al*. 2022; Wu *et al*. 2017; Zhu *et al*. 2021), the feeding speed is selected to be a constant value of 0.35 m/s. The measurement and control system consists of transmitter 24V DC power supply, data acquisition board (MCC-1608G acquisition card, sampling rate 250 ks/s), S-type tension pressure sensor, and computer. A data acquisition module and software (DAQami) is used to capture the amplified signals (MCC 1608G). The technical parameters of the cutting test bench are shown in Table 1.

Table 1. Technical Parameters of Cutting Test Bench

Parameters	Numerical Value
Average cutting speed (m·s^{-1})	0.2 to 1
AC motor power (kW)	2.2
S-type tension sensor (kg)	±500kg
Sampling frequency (Hz)	1000
Maximum data acquisition channels	8

Data Acquisition and Processing

The *F*-value affects the cutting edge life and the *E* value is decisive for the power selection of the cutting device (Oraby and Hayhurst 2004; Li *et al*. 2020; Nasir and Cool 2021). Therefore, both *F* and *E* were selected as target values.

Figure 2 shows the typical cutting force curve of the branch with time. Because the C.K. branch is a plant fiber body, there is a pre-pressure elastic deformation process during the cutting process, resulting in a longer time required for the cutting force to rise to the peak than to fall. The mechanical properties of cutting are similar to those of cotton straw and apple branches (Aydin *et al*. 2018; Kang *et al*. 2020). The peak of the curve is taken as the *F* value, which reflects the maximum resistance of the branch cutting process. The *E* value is obtained by integrating the variation of the force curve with the cutting speed,

$$E = \int_0^t F \cdot v \, dt \tag{1}$$

where *E* is the cutting energy consumption (J), *t* is the cutting time (s), *F*(t) is the cutting force curve (N), and *v* is the average cutting speed (m/s).
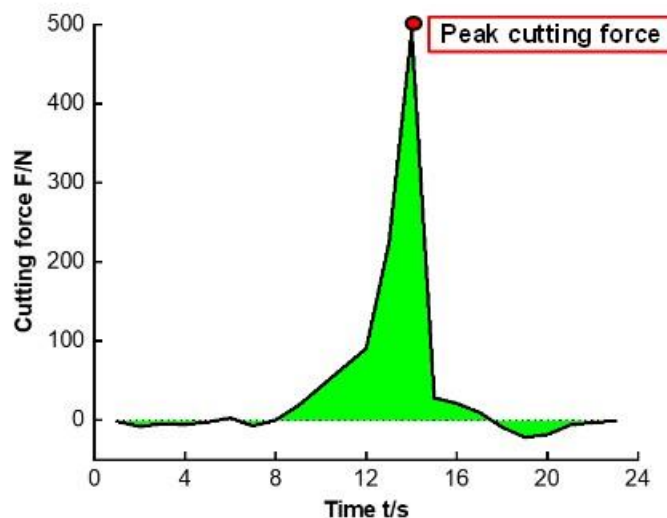
Fig. 2. Typical cutting force curve of the branch with time

After the cutting test was completed, the remaining part of the branches was sealed and labeled with plastic wrap immediately. The *W* of the branches was determined by the drying method according to standard protocols (GB/T 1931-2009.). The *W* of fresh branches was measured to be 27.3% to 32.4%.

Single-factor Test

To investigate the effects of each test factor on the *F* and *E* values of branches, the six sets of single-factor tests were designed for *D*, *v*, *c*, *β*, *λ*, and *W*. Because the diameter of C.K. branches growing for 3 to 5 years usually does not exceed 12 mm (Gao *et al*. 2021), the range of *D* was taken to be 8 to 20 mm to study the relationship between branch diameter and target value. In the other groups of experiments, the *D* was selected to be 10 to 12 mm. Due to the limitations of the test conditions, there is an operational risk when the *v* is high, so the *v* was taken as 0.2 to 0.8 m/s in the single-factor test of the *v*. In other groups of tests, the *v* was taken as 0.4 m/s. When the *c* is small, the friction between the tool and the branch intensifies and affects the service life of the tool (Kang *et al*. 2020; Xiao *et al*. 2021). When the *c* is large, the cutting force increases sharply. Therefore, the range of the *c* was 0.1 to 3 mm, and a total of 4 levels were set. In the other group tests, the *c* was taken as 1 mm. The *β* value determines the strength of the blade, and when the *β* is small, chipping is very likely to occur (Spagnoli *et al*. 2019; Kuhn *et al*. 2020). Therefore, the *β* value was set to 20° to 35°, and the level was set at 5° intervals. The *β* value was taken as 25° when conducting other groups of tests. The *λ* value of the tool affects the mechanical properties of branch cutting. The *λ* value will cause the branch to slip off when it is larger, but the *λ* value will increase the branch cutting force when it is smaller (Johnson *et al*. 2012; Gao *et al*. 2021). Therefore, the value range of the *λ* was taken from 5° to 20°, and a total of 4 levels were set. In other groups of tests, the *λ* was taken as 20°. The average moisture content of branches was measured to be 20.7%, 14.2%, and 10.5% after the branches were placed in the laboratory room (23 ± 0.5°C) for 2, 4, and 8 days, respectively. A single-factor test for *W* was performed at each of these four moisture contents. In other groups of tests, the test subjects were fresh branches. The test factors and levels are shown in Table 2. Each test group was conducted 5 times.

Table 2. Single-factor Test Factors and Levels

Level	*v* (m/s)	*c* (mm)	*β* (°)	*λ* (°)	*W* (%)
1	0.2	0.1	20	5	29.8
2	0.3	1	25	10	20.7
3	0.4	2	30	15	14.2
4	0.5	3	35	20	11.5
5	0.6				
6	0.7				
7	0.8				

Multi-Factor Test

Based on the single-factor test, the *F* and *E* as the target values, and the *v*, *c*, *β*, and *λ* as the test factors were studied based on the Box-Behnken response surface test design principle (Jiang *et al*. 2021; Xie *et al*. 2022). Analysis of variance (ANOVA) was performed on the test results using Design-Expert R11 (Stat-Ease, Minneapolis, MN, USA). The test factors and levels are shown in Table 3, with five replications of each level test. The *D* was 10 to 12 mm, and the *W* of the branches was 28.6 to 31.7%.

bioresources.com

Table 3. Multi-factor Tests and Levels

Test Factors	Coded Level		
	-1	0	1
v (m/s)	0.3	0.4	0.5
c (mm)	1	1.5	2
β (°)	25	30	35
λ (°)	10	15	20

RESULTS AND DISCUSSION

Analysis of Single-Factor Test Results

Branch diameter D

As shown in Fig. 3a, the F and E values in general increased sharply with the increase of D. The D is directly related to the number of fibers, and the majority of the cutting energy consumption is used to cut the fibers (Meng *et al*. 2019; Gao *et al*. 2021). Therefore, the number and intensity of the fibers inside the branch determine the power consumption of the blade.

Average cutting speed v

As shown in Fig. 3b, the F decreased with the increase of the v and then it smoothly changed. The E showed a trend of decreasing and then increasing with the increased v.

The C.K. branches are anisotropic, non-linear composite plant fiber material, and the cutting process is divided into the extrusion deformation stage and the cutting stage (Che *et al*. 2022). When the v is slower ($v < 0.4$ m/s), the branch undergoes a larger compressive deformation. As the v increases, the branch cutting point transfer deformation time gradually decreases, and the compression deformation of the branch by the blade gradually decreases (Kang *et al*. 2020). At this time, the branch changes from the extrusion stage to the cutting stage, and the F and E gradually decrease. When the v exceeds 0.5 m/s and continues to increase, the time of blade transfer deformation no longer changes significantly (Mathanker *et al*. 2015). Therefore, the changing trend of the F is gradually smooth, and then the E shows an increasing trend with the increase of the v.

Cutting clearance *c*

With the increase of the c, the F showed a trend of decreasing and then increasing. The F was the smallest at the c of 1 mm, and the cutting quality was the best (Fig. 3c). When the c was too small or too large, the absolute value of the difference between the ratio of shear zone and fracture zone was larger, and the F value was larger. While the c was 1 mm, the shear band ratio and fracture band ratio complemented each other, so the F value was the smallest. The cutting sections with different cutting gaps are shown in Fig. 4.

As shown in Fig. 5, the branch is subjected to the forces F_1 and F_2 of the moving knife and the fixed knife in the cutting process. As the t exists, the branch is subjected to the torque M. When the c is less than 0.5 mm, the torque M is small, and the friction between the blade and the wood chips is increased, which makes the E increase (Xu 2013; Wargula *et al*. 2022). However, when the t is greater than 1.5 mm, the branch is subjected to a larger torque M, so that the cutting process is broken off to produce a step-like feature. Therefore, the E with the increase of the c shows a trend of decreasing and then increasing.

bioresources.com

Peak cutting force — The fitting curve of peak cutting force — 95% confidence band of peak cutting force — 95% prediction band of peak cutting force

Cutting energy consumption — The fitting curve of cutting energy — 95% confidence band of cutting energy — 95% prediction band of cutting energy

Note: *v* of 0.4m/s; *c* of 1mm; β of 25°; λ of 20°; *W* of 27.3 to 31.1%

Note: D of 10 to 12mm; *c* of 1mm; β of 25°, λ of 20°; *W* of 27.5 to 31.7%

Note: D of 10 to 12mm; *v* of 0.4m/s; β of 25°; λ of 20°; *W* of 27.4 to 32.0%

Note: D of 10 to 12mm; *v* of 0.4m/s, *c* of 1mm; λ of 20°; *W* of 27.9 to 32.2%

Note: D of 10 to 12mm; *v* is 0.4m/s, *c* of 1mm; β of 25°; *W* of 28.1 to 32.4%

Note: D of 10 to 12mm; *v* of 0.4m/s, *c* of 1mm; β of 25°; λ of 20°

Fig. 3. Single-factor test results

Wedge angle β

In the cutting test, the branches were cut smoothly in one pass when the *β* was 5 to 20°. As shown in Fig. 3d, the *F* increased with increasing *β*. A smaller *β* indicated easier cutting of the fiber structure inside the branch. The *β* value determines the strength of the cutting edge, which affects the service life of the blade (Song *et al*. 2022). The relationship between wedge angle and service life needs to be considered when designing cutting blades. The *E* value tended to decrease and then increase with the increase of *β*. Because C.K. is a viscoelastic material (Zhang *et al*. 2019), the *E* value is related to the cohesive force of the plant.

| t=0.1mm | t=1mm | t=2mm | t=3 mm |

Fig. 4. The cutting sections with different cutting clearance

1-Fixed blade; 2-Moving blade; 3-Branch
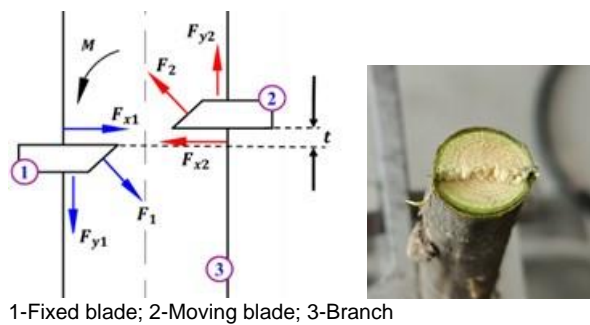
Fig. 5. Schematic diagram of the forces during the cutting of the branch

Tool cutting edge inclination angle λ

As shown in Fig. 3e, when the blade is cutting the branch, a larger *λ* indicates a smaller actual wedge angle of the blade cutting into the branch. The required normal force decreased, and the *F* and *E* decreased. When the *λ* value is too large, the relative travel between the branch and the blade increases, so that the frictional power consumption increases. Although the *F* is reduced, the effect of frictional power consumption is more significant (Ding *et al*. 2015). Therefore, the *E* shows an increasing trend after the change. As shown in Fig. 6, the different bevel angles cause the blade with different dynamic wedge angles when cutting the branches, which are geometrically analyzed as follows,

$$\tan \beta = \frac{l_{CD}}{l_{OD}} \quad \tan \beta' = \frac{l_{AB}}{l_{OB}} \quad l_{OB} = \frac{l_{OD}}{\cos \lambda_s} \tag{3}$$

such that $\tan \beta' = \tan \beta \cos \lambda_s$, $\beta' < \beta$. During the entry of the cutter into the material, the dynamic wedge angle of the slip cut is smaller than that of the forward cut, so the slip cut has less cutting resistance (Orlowski *et al.* 2013, 2020). Oblique cutting should be used as much as possible during branch cutting to reduce cutting resistance and power consumption (Johnson *et al*. 2012; Wargula *et al*. 2022).

Moisture content W

As shown in Fig. 3f, the *F* and *E* values of the branches decreased with increasing *W*. As the *W* increases, the dry matter decreases, the toughness of branches decreases, and the ultimate stress decreases, which makes the *F* and *E* of branches decrease. Therefore, it is recommended to crush and cut the fresh branches to help reduce the cutting energy.
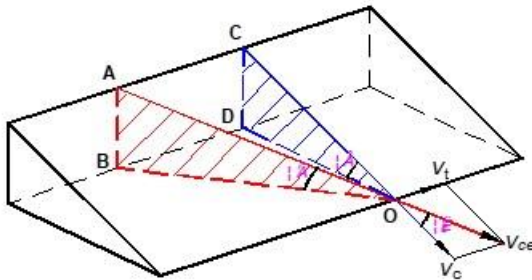
Fig. 6. Oblique cutting principle

Analysis of Multi-Factor Test Results

Regression modeling and significance testing

The results of the multi-factor experiments are shown in Table 4.

Table 4. Test Results

Serial Number	Test Factors				Test Objective	
	v (m/s)	*c* (mm)	*β* (°)	*λ* (°)	*F* (N)	*E* (J)
1	0.3	1	30	15	763.7	9.6
2	0.5	1	30	15	672.3	7.3
3	0.3	2	30	15	793.8	12.3
4	0.5	2	30	15	695.2	10.4
5	0.4	1.5	25	10	726.9	8.1
6	0.4	1.5	35	10	756.6	10.4
7	0.4	1.5	25	20	714.3	6.9
8	0.4	1.5	35	20	748.1	9.5
9	0.3	1.5	30	10	751.8	9.7
10	0.5	1.5	30	10	725.7	8.3
11	0.3	1.5	30	20	783.2	9.1
12	0.5	1.5	30	20	694.3	7.2
13	0.4	1	25	15	678.5	8.8
14	0.4	2	25	15	742.4	9.3
15	0.4	1	35	15	737.2	8.4
16	0.4	2	35	15	771.6	11.5
17	0.3	1.5	25	15	709.3	8.7
18	0.5	1.5	25	15	664.8	6.1
19	0.3	1.5	35	15	766.1	9.8
20	0.5	1.5	35	15	695.7	8.4
21	0.4	1	30	10	762.9	8.9
22	0.4	2	30	10	779.5	10.5
23	0.4	1	30	20	703.4	7.3
24	0.4	2	30	20	756.8	9.5
25	0.4	1.5	30	15	728.4	9.3
26	0.4	1.5	30	15	712.7	8.8
27	0.4	1.5	30	15	720.3	8.5
28	0.4	1.5	30	15	698.4	8.1
29	0.4	1.5	30	15	709.1	9.2

From the analysis in Table 5, the p-values of the response surface models for *F* and *E* were less than 0.0001, indicating that the regression models were highly significant. The P-values of the lack of fit terms were greater than 0.05 (0.2955 and 0.3471, respectively), indicating that the experimental errors were small and the regression equations obtained were well fitted. The coefficients of determination R^2 were 0.9161 and 0.9028, which show high fitting accuracy, indicating that the model could analyze the degree of influence of each factor and predict the optimal value within the range of the test values.

Table 5. Analysis of Variance

Source	df	SS	MS	F-value	p-value
Peak cutting force *F*(N)					
Model	14	31305.16	2236.08	10.92	< 0.0001
v	1	14693.00	14693.00	71.75	< 0.0001
c	1	4081.14	4081.14	19.93	0.0005
β	1	4764.07	4764.07	23.27	0.0003
λ	1	889.24	889.24	4.34	0.0560
v·c	1	12.96	12.96	0.0633	0.8050
v·β	1	167.70	167.70	0.8190	0.3808
v·λ	1	985.96	985.96	4.82	0.0456
c·β	1	217.56	217.56	1.06	0.3201
c·λ	1	338.56	338.56	1.65	0.2194
β·λ	1	4.20	4.20	0.0205	0.8881
v^2	1	1.56	1.56	0.0076	0.9317
c^2	1	1915.62	1915.62	9.36	0.0085
$β^2$	1	7.02	7.02	0.0343	0.8558
$λ^2$	1	3419.43	3419.43	16.70	0.0011
Residual	14	2866.75	204.77		
Lack of fit	10	2350.89	235.09	1.82	0.2955
Pure error	4	515.87	128.97		
Total	28	34171.91			
R^2 =91.61%					
Cutting energy *E*(J)					
Model	14	45.67	3.26	9.29	< 0.0001
v	1	11.02	11.02	31.39	< 0.0001
c	1	14.52	14.52	41.35	< 0.0001
β	1	8.50	8.50	24.21	0.0002
λ	1	3.41	3.41	9.72	0.0076
v·c	1	0.04	0.04	0.114	0.7407
v·β	1	0.36	0.36	1.03	0.3284
v·λ	1	0.063	0.063	0.178	0.6795
c·β	1	1.69	1.69	4.81	0.0456
c·λ	1	0.09	0.09	0.256	0.6205
β·λ	1	0.023	0.023	0.064	0.8038
v^2	1	0.005	0.005	0.014	0.9076
c^2	1	4.52	4.52	12.88	0.0030
$β^2$	1	0.151	0.151	0.429	0.5228
$λ^2$	1	0.299	0.299	0.854	0.3711
Residual	14	4.92	0.351		
Lack of fit	10	3.93	0.393	1.59	0.3471
Pure error	4	0.988	0.247		
Total	28	50.59			
R^2=89.26%					

For the F model, the regression terms of v, c, β, c^2, and λ^2 (P<0.01) showed highly significant effects, and the regression term of $v \cdot \lambda$ (P<0.05) had a significant effect. For the E model, the regression terms v, c, β, λ, and c^2 (P<0.01) had a highly significant effect, and the $c \cdot \beta$ (P<0.05) regression term has a significant effect. The p-value of the other terms was all greater than 0.05, indicating that the effect on the regression model was not significant.

The simplified regression models of F and E were obtained by stepwise regression analysis, removing the insignificant terms, as follows:

$$F = -34.99v + 18.44c + 19.93\beta - 8.61\lambda - 15.70v \cdot \lambda + 17.43c^2 + 23.20\lambda^2 + 712.95 \tag{6}$$

$$E = -0.96v + 1.10c + 0.84\beta - 0.53\lambda + 0.65c \cdot \beta - 0.89c^2 + 8.47 \tag{7}$$

Effect of interaction terms on branch cutting

The $v \cdot \lambda$ and $c \cdot \beta$ interaction terms have interactive effects on the F and E, respectively. As shown in Fig. 7a, the F value decreased linearly with the increase of the v. When the λ was 0 to 13°, as the tool cutting edge inclination angle produced a slip-cutting effect. The larger the blade λ, the smaller the actual wedge angle of the blade edge when cutting branches, which makes the cutting force decrease (Vu *et al.* 2020). When the λ continues to increase, the cutting stroke of the blade increases, which makes the frictional resistance become the main factor affecting the cutting force, making the cutting force gradually increase (Kang *et al.* 2020; Gao *et al.* 2021). When the v is 0.3 to 0.5 m/s, as the v increases, the elastic deformation time of the branch decreases, which makes the cutting force gradually decrease (Kakahy *et al.* 2014).
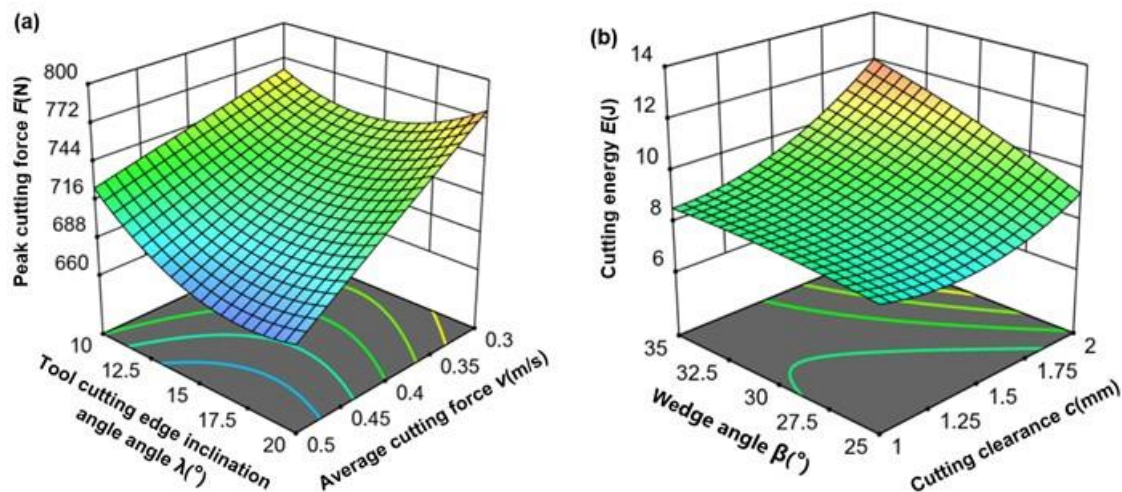
Fig. 7. Effect of interaction terms on branch cutting

As shown in Fig. 7b, the E value increased with the increase of β. With the increase in c, the E value showed a trend of decreasing and then increasing. Within v values of 0.3 to 0.5 m/s, the c and β were the main influences on the peak cutting force. When the c was small, the friction between the blade and the cross-section increased, making the E increase (Ghahraei *et al.* 2011; Zhang *et al.* 2019). When the c is large, significant torque will be generated between the two blades, which makes the branch break during the cutting process. The branch is broken in a step-like manner, making the E value increase sharply

(Gao *et al.* 2021). When the β value is reduced, the blade is sharp and more likely to damage the internal fiber structure of the branch. Therefore, when designing and optimizing the branch cutting device, the test factors affecting the *F* and *E* need to be taken into account.

Parameter Optimization

To achieve the best cutting performance, it is essential to require low *F* and *E* values of the branches. Because the influence of each factor on the test objective varies, multi-objective optimization was performed to find the best combination of parameters to satisfy the cutting performance.

According to the actual operating conditions, the multi-objective parametric optimization analysis is performed with the constraints as follows:

$$\begin{cases} 1.0mm \leq c \leq 2.0mm \\ 25^\circ \leq \beta \leq 35^\circ \\ 0.3m/s \leq v \leq 0.5m/s \\ 10^\circ \leq \lambda \leq 20^\circ \\ \min(f(v,c,\beta,\lambda), E(v,c,\beta,\lambda)) \end{cases} \tag{8}$$

The optimized combination of cutting parameters was obtained with *v* of 0.49 m/s, *c* of 1.37 mm, β of 25.01°, and λ of 19.99° using Design-Expert software. The *F* value was 654.14 N and *E* was 6.20 J under this combination of cutting parameters.

Testing Verification

To verify the accuracy of the model prediction, five replicate experiments were conducted on the cutting test bench using the above parameter combinations. Considering the feasibility of the experiment, the combination of cutting parameters was set to *v* of 0.5 m/s, *c* of 1.4 mm, β of 25°, and λ of 20°. With the optimized scheme, the experiments were conducted, and the results are shown in Table 5. The errors between the target values of the prediction model and the measured target values under the optimal parameter combination were less than 5%, which verified that the model was reliable.

Table 6. Measured Values of Each Target Value with Optimized Conditions

Test Number	Peak Cutting Force *F* (N)	Cutting Energy Consumption *E* (J)
1	663.5	5.92
2	652.9	5.53
3	647.4	6.48
4	640.8	5.79
5	645.3	5.77
Average	644.38	5.90
Relative error /%	1.5%	4.8%

CONCLUSIONS

1. When the average cutting speed v is larger or the α value is smaller, the peak cutting force F can be reduced, but the cutting energy consumption E will gradually increase.

2. The results of the single-factor test show that the F and E increased with the increase of branch diameter D, which gradually decreased with the increase of moisture content W. When the v was 0.1 to 0.8 m/s, the F decreased gradually with the increase of the v. The E value showed a trend of decreasing and then increasing with the increase of v. When the cutting clearance value c was 0.1 to 3 mm, the F and E showed a trend of decreasing and then increasing with the increase of the c. When the wedge angle β was 20 to 35°, the F value gradually increased with the increase of the β, and E showed a trend of decreasing and then increasing with the increase of the β. When the tool cutting edge inclination angle λ was 0 to 20°, the F and E values showed a trend of decreasing and then increasing with the increase of λ.

3. The Box-Behnken center combination test method was used to optimize the model of F and E, which resulted in the best combination of cutting parameters with v of 0.5 m/s, c of 1.4 mm, β of 25°, and λ of 20°. With the optimal combination of parameters, the F value was 654.14 N and E was 6.20 J. The accuracy of the model and the optimization results were verified through tests, and the relative errors were less than 5%, indicating that the model was highly reliable. It can provide data support for the subsequent development of low-power and high-efficiency cutting equipment.

ACKNOWLEDGMENTS

REFERENCES CITED

Atkins, A. G. (2009). *The Science and Engineering of Cutting. The Mechanics and Process of Separating, Scratching and Puncturing Biomaterials, Metals and Non-Metals*, Butterworth-Heinemann, an imprint of Elsevier, Oxford.

Aydin, I., and Arslan, S. (2018). "Mechanical properties of cotton shoots for topping," *Ind. Crop. Prod.* 112, 396-401. DOI: 10.1016/j.indcrop.2017.12.036

Che, C.W., Xiao, S. C., Ding, A. J., Peng, X. M., and Su, J. R. (2022). "The characteristics of radial growth and ecological response of *Caragana korshinskii* Kom. under different precipitation gradient in the Western Loess Plateau, China," *Front. Plant Sci.* 13. DOI: 10.3389/fpls.2022.862529

Cristovao, L., Ekevad, M., and Gronlund, A. (2013). "Industrial sawing of *Pinus sylvestris* L.: Power consumption," *BioResources* 8(4), 6044-6053. DOI: 10.15376/biores.8.4.6044-6053

Ding, S., Xue, X., Cai, C., Cui, L., and Chen, C. (2015). "Optimization and experiment of blade parameter for pear branches cutting device," *Transactions of the Chinese Society of Agricultural Engineering* 31, 75-82. DOI: 10.11975/j.issn.1002-6819.2015.z2.011

Esgici, R. (2020). "The effect of knife type on cutting characteristics of cotton stalk," *Fresen. Environ. Bull.* 29, 2772-2777.

Gan, H., Mathanker, S., Momin, M. A., Kuhns, B., Stoffel, N., and Hansen, A., Grift, T. (2018). "Effects of three cutting blade designs on energy consumption during mowing-conditioning of Miscanthus Giganteus," *Biomass Bioenerg.* 109, 166-171. DOI: 10.1016/j.biombioe.2017.12.033

Gao, Y., Wang, Y., Qu, A., Kan, J., Kang, F., and Wang, Y. (2022). "Study of sawing parameters for *Caragana korshinskii* (C.K.) branches," *Forests.* 13. DOI: 10.3390/f13020327

Gao, Y. Y., Kang, F., Kan, J. M., Wang, Y. T., and Tong, S. Y. (2021). "Analysis and experiment of cutting mechanical parameters for *Caragana korshinskii* (C.k.) branches," *Forests* 12. DOI: 10.3390/f12101359

GB/T 1299-2014. (2014) "Tool and mould steels, inspection methods of microstructure for metals," Standardization Administration of China, Beijing, China.

GB/T 1931-2009. (2009) "Method for determination of the moisture content of wood," Standardization Administration of China, Beijing, China.

Ghahraei O, Ahmad D, Khalina A, Suryanto H, and Othman, J. (2011). "Cutting tests of kenaf stems," *T Asabe* 54(1), 51-56.

Jiang, Q. J., He, Z. L., Wang, Y. W., and Wang, J. (2021). "Optimizing the working performance of a boat-type tractor using central composite rotatable design and response surface method," *Comput. Electron. Agr.* 181. DOI: 10.1016/j.compag.2020.105944

Johnson, P. C., Clementson, C. L., Mathanker, S. K., Grift, T. E., and Hansen, A. C. (2012). "Cutting energy characteristics of Miscanthus x giganteus stems with varying oblique angle and cutting speed," *Biosyst. Eng.* 112, 42-48. DOI: 10.1016/j.biosystemseng.2012.02.003.

Kakahy, A., Ahmad, D., Akhir, M., Sulaiman, S., and Ishak, A. (2014). "Effects of knife shapes and cutting speeds of a mower on the power consumption for pulverizing sweet potato vine," *Key Engineering Materials* (594–595), 1126-1130. DOI: 10.4028/www.scientific.net/kem.594-595.1126

Kang, F., Tong, S., Zhang, H., Li, W., Chen, Z., and Zheng, Y. (2020). "Analysis and experiments of reciprocating cutting parameters for apple tree branches," *Transactions of the Chinese Society of Agricultural Engineering* 36, 9-16. DOI: 10.11975/j.issn.1002-6819.2020.16.002

Kuhn, F., Lopenhaus, C., Brimmers, J., Klocke, and F., Bergs, T. (2020). "Analysis of the influence of the effective angles on the tool wear in gear hobbing," *Int. J. Adv. Manuf. Tech.* 108, 2621-2632. DOI: 10.1007/s00170-020-05499-0

Li, Z. P., Zhang, C., and Wang, B. N. (2020). "Research on design of blueberry picker based on vibration strategy," *Forest Engineering* 36(2), 55-61. DOI: 10.16270/j.cnki.slgc.2020.02.009

Liu, J. M., Zhao, D., and Zhao, J. (2020). "Study of the cutting mechanism of oil tree peony stem," *Forests.* 11. DOI: 10.3390/f11070760

Mathanker, S. K., Grift, T. E., and Hansen, A. C. (2015). "Effect of blade oblique angle and cutting speed on cutting energy for energycane stems," *Biosyst. Eng.* 133, 64-70. DOI: 10.1016/j.biosystemseng.2015.03.003

Meng, Y. M., Wei, J. D., Wei, J., Chen, H., and Cui, Y. S. (2019). "An ANSYS/LS-DYNA simulation and experimental study of circular saw blade cutting system of mulberry cutting machine," *Comput. Electron. Agr.* 157, 38-48. DOI:

10.1016/j.compag.2018.12.034

Nasir, V., and Cool, J. (2021). "Cutting power and surface quality in sawing kiln-dried, green, and frozen hem-fir wood," *Wood Sci. Technol.* 55, 505-519. DOI: 10.1007/s00226-020-01259-1

Oraby, S. E., and Hayhurst, D. R. (2004). "Tool life determination based on the measurement of wear and tool force ratio variation," *Int. J. Mach. Tool. Manu.* 44, 1261-1269. DOI: 10.1016/j.ijmachtools.2004.04.018

Orlowski, K. A., Ochrymiuk, T., Atkins, A., and Chuchala, D. (2013). "Application of fracture mechanics for energetic effects predictions while wood sawing," *Wood Sci Technol.* 47(5), 949-963. DOI: 10.1007/s00226-013-0551-x

Orlowski, K. A., Ochrymiuk, T., and Hlaskova, L. (2020). "Revisiting the estimation of cutting power with different energetic methods while sawing soft and hard woods on the circular sawing machine: A Central European case," *Wood Sci Technol.* 54(2), 457-477. DOI:10.1007/s00226-020-01162-9

Qiu, M. M., Meng, Y. M., Li, Y. Z., and Shen, X. B. (2021). "Sugarcane stem cut quality investigated by finite element simulation and experiment," *Biosyst. Eng.* 206, 135-149. DOI: 10.1016/j.biosystemseng.2021.03.013

Song, S. Y., Zhou, H. P., Xu, L. Y., Jia, Z. C., and Hu, G. M. (2022). "Cutting mechanical properties of sisal leaves under rotary impact cutting," *Ind. Crop. Prod.* 182. DOI: 10.1016/j.indcrop.2022.114856

Spagnoli, A., Brighenti, R., Terzano, M., and Artoni, F. (2019). "Cutting resistance of soft materials: Effects of blade inclination and friction," *Theor. Appl. Fract. Mec.* 101, 200-206. DOI: 10.1016/j.tafmec.2019.02.017

Suzuki, K., Tsuji, N., Shirai, Y., Hassan, M. A., and Osaki, M. (2017). "Evaluation of biomass energy potential towards achieving sustainability in biomass energy utilization in Sabah, Malaysia," *Biomass Bioenerg.* 97, 149-154. DOI: 10.1016/j.biombioe.2016.12.023

Vu, V. D., Ngo, Q. H., Nguyen, T. T., Nguyen, H. C., Nguyen, Q. T., and Nguyen, V. D. (2020). "Multi-objective optimisation of cutting force and cutting power in chopping agricultural residues," *Biosyst. Eng.* 191, 107-115. DOI: 10.1016/j.biosystemseng.2020.01.007

Vu, V. D., Nguyen, T. T., Chu, N. H., Ngo, Q. H., Ho, K. T., and Nguyen, V. D. (2020). "Multiresponse optimization of cutting force and cutting power in chopping agricultural residues using grey-based Taguchi method," *Agriculture-Basel* 10. DOI: 10.3390/agriculture10030051

Wang, F. L., Ma, S. C., Xing, H. N., Bai, J., Ma, J. Z., Hu, J. W., and Yang, Y. Z. (2021). "High-speed photography analysis on sugarcane base cutting process of contra-rotating basecutters," *Sugar Tech.* 23, 1118-1125. DOI: 10.1007/s12355-020-00942-8.

Wang, T. T., Zheng, J. Y., Liu, H. T., Peng, Q., Zhou, H. M., and Zhang, X. C. (2021). "Adsorption characteristics and mechanisms of Pb^{2+} and Cd^{2+} by a new agricultural waste-*Caragana korshinskii* biomass derived biochar," *Environ. Sci. Pollut. R.* 28, 13800-13818. DOI: 10.1007/s11356-020-11571-9

Wargula, L., Kukla, M., Wieczorek, B., and Krawiec, P. (2022). "Energy consumption of the wood size reduction processes with employment of a low-power machines with various cutting mechanisms," *Renew. Energ.* 181, 630-639. DOI: 10.1016/j.renene.2021.09.039.

Waseem, M., Nie, Z. F., Yao, G. Q., Hasan, M., Xiang, Y., and Fang, X. W. (2021). "Dew absorption by leaf trichomes in *Caragana korshinskii*: An alternative water

acquisition strategy for withstanding drought in arid environments," *Physiol. Plantarum* 172, 528-539. DOI: 10.1111/ppl.13334

Wu, B., Wang, D., Wang, G., Fu, Z., and Kang, C. (2017). "Optimization and experiments of cut-condition device working parameter on mower conditioner," *Trans. Chin. Soc. Agric. Mach*. 48, 76-83. DOI:10.6041/j.issn.1000-1298.2017.10.009.

Xiao, X., Huang, J. J., Li, M., Xu, Y. W., and Zhang, H. D. (2021). "Parameter analysis and experiment of citrus stalk cutting for robot picking," *Eng. Agr.* 41, 551-558. DOI: 10.1590/1809-4430-Eng.Agric.v41n5p551-558/2021

Xie, L. X., Wang, P., Luo, J., Yi, W. Y., and Deng, J. (2022). "Optimisation and numerical simulation of shearing blade used for citrus seedling grafting," *Biosyst. Eng.* 215, 67-79. DOI: 10.1016/j.biosystemseng.2022.01.006

Xu, H., Wang, Z. J., Li, Y., He, J. L., and Wu, X. D. (2020). "Dynamic growth models for *Caragana korshinskii* shrub biomass in China," *J. Environ. Manage.* 269. DOI: 10.1016/j.icarus.2020.110675

Xu, S. Y. (2013). "Waste tire crushing and shearing machine tools working methods of the gap," *Advanced Materials Research* 823, 309-312. DOI: 10.4028/www.scientific.net/AMR.823.309

Zhang, C. L., Chen, L. Q., Xia, J. F., and Zhang, J. M. (2019). "Effects of blade sliding cutting angle and stem level on cutting energy of rice stems," *International Journal of Agricultural and Biological Engineering* 12, 75-81. DOI: 10.25165/j.ijabe.20191206.4604

Zhang, L., Tong, S. Y., and Kang, F. (2022). "Analysis and experiments of cutting blade parameters for grape branches," *Forest Engineering* 38(2), 95-104. DOI: 10.16270/j.cnki.slgc.2022.02.012

Zhang, J., Zheng, D. C., Wu, K., and Zhang, X. Q. (2019). "Combustion characteristics of *Caragana korshinskii* Kom," *J. Biobased Mater. Bio.* 13, 69-78. DOI: 10.1166/jbmb.2019.1827

Zhu, L., Wang, D., You, Y., Wu, B., Ma, W., and Huan, X. (2021). "Design and experiment of crawler-type grass belt harvester in forest," *Trans. Chin. Soc. Agric. Mach.* 52, 126-133. DOI: 10.6041/j.issn.1000-1298.2021.04.013.